TÜBİTAK

Turkish Journal of Chemistry

http://journals.tubitak.gov.tr/chem/

Research Article

Turk J Chem
(2019) 43: 1170 – 1182

doi:10.3906/kim-1903-74

Acetyl- and butyrylcholinesterase inhibitory activity of selected photochemically synthesized polycycles

Ivana ŠAGUD[1], Irena ŠKORIĆ[1], Dragana VUK[1], Ana RATKOVIĆ[1], Franko BURČUL[2,*]
[1]Department of Organic Chemistry, Faculty of Chemical Engineering and Technology, University of Zagreb, Zagreb, Croatia
[2]Department of Analytical Chemistry, Faculty of Chemistry and Technology, University of Split, Split, Croatia

Received: 28.03.2019 • **Accepted/Published Online:** 14.06.2019 • **Final Version:** 06.08.2019

Abstract: Alzheimer's disease (AD) is a progressive neurodegenerative disorder and the main cause of dementia in the elderly population. Since the treatment of AD has been associated with the activity of acetylcholinesterase (AChE) and butyrylcholinesterase (BChE), their inhibitors remain the main focus of AD investigations. In this study we evaluated cholinesterase inhibitory activity of 14 bicyclo[3.2.1]octene/octadiene derivatives and naturally occurring sesquiterpene alcohol cedrol. These 14 compounds have been efficiently and ecologically prepared by a photochemical approach in batch photochemical reactors. Various compounds with the bicyclo[3.2.1]octene skeleton have already been successfully evaluated for treatment of central nervous system disorders and AD. Among the tested polycyclic derivatives, compounds 4-[(9*S*)-tricyclo[6.3.1.0^{2,7}]dodeca-2,4,6,10-tetraen-9-yl]pyridine (**3**) and (11*S*)-11-(4-chlorophenyl)-12-[(*E*)-2-(4-chlorophenyl)ethenyl]tricyclo[6.3.1.0^{2,7}]dodeca-2,4,6,9-tetraene (**6**) showed the best inhibitory activity on BChE (IC_{50} = 8.8 μM) and AChE (IC_{50} = 17.5 μM), respectively.

Key words: Acetylcholinesterase inhibition, butyrylcholinesterase inhibition, benzobicyclo[3.2.1]octenes, benzobicyclo[3.2.1]octadienes, polycycles

1. Introduction

Alzheimer's disease (AD) is one of the most common neurodegenerative disorders and causes of dementia in Western society, mostly affecting the elderly population. The World Health Organization (WHO) estimates that AD affects over 50% of people older than 85 [1–3]. The most prominent symptom of this disease is a progressive decrease in cognitive function, which in turn leads to changes in behavioral patterns and a decrease in the functional capacity of the affected individuals. Low concentrations of the acetylcholine (ACh) neurotransmitter in the brain and the genesis of amyloid plaques are considered as the hallmarks of AD. Acetylcholinesterase (AChE, EC 3.1.1.7) plays a fundamental role in the unaffected cholinergic synapses by hydrolyzing the ACh and terminating the neurotransmission, and while butyrylcholinesterase (BChE, EC 3.1.1.8) function remains elusive, it can act as a surrogate in the case of AChE deficiency [3,4]. Since the amyloid plaque decrease and ACh concentration increase are both connected to the AChE and BChE enzymes, an inhibitor that could inhibit both of these enzymes would be useful [5]. Inhibition of these enzymes currently represents the backbone of AD pharmacotherapy that is able to increase the neurotransmitter ACh in the brain and decrease amyloid plaque. Hence, the search for novel cholinesterase (ChE) inhibitors remains crucial for the treatment of AD [3,6–9].

*Correspondence: franko@ktf-split.hr

Although AChE and BChE are encoded on different chromosomes they show 65% amino acid sequence homology and they contain a catalytic triad that comprises the amino acid residues of serine (Ser), histidine (His), and glutamic acid (Glu), which are located at the bottom of a 20-Å gorge [10–12]. The active site of AChE is a deep, narrow gorge (300 $Å^3$), while the active site of BChE looks more like a bowl (500 $Å^3$) and contains about 40% fewer aromatic residues than that of AChE, which are substituted with smaller aliphatic or even polar residues [4]. The amino acids lining this gorge seem to determine the substrate selectivity as the entryway to AChE is narrower than that to BChE. This is mainly due to the aromatic residues Tyr-124 and Trp-286, which are located at the gorge entrance and which are occupied by glutamine (Gln-119) and alanine (Ala-277) in BChE. Inside the gorge, there is a difference in the acyl binding site residues, which in AChE consist of two aromatic phenylalanine residues (Phe-295 and Phe-297), while BChE contains the smaller aliphatic residues leucine (Leu-286) and valine (Val-288) [11,12]. All of this allows BChE to bind bulkier substrates into the active site. Tyrosine (Tyr-337) (Ala-328 in BChE) in AChE also hinders bulkier substrates from interacting with the catalytic triad.

The bicyclo[3.2.1]octane skeleton is a common subunit in many natural products. It is present in diterpene families of compounds, such as the kaurenes and the gibberellins, and also in many sesquiterpenes [13]. One of the more interesting properties of the bicyclo[3.2.1]octane skeleton is its rigidity, which promotes specific coordination of two or more ligands on it, which can be of great value to medicinal chemists in the search for biological activity [14–17]. This structural moiety forms a basic framework of numerous biologically active natural compounds and their metabolites [18–20]. More importantly, compounds with the bicyclo[3.2.1]octene skeleton are proving to be potent inhibitors of dopamine and serotonin transporters and also play a crucial role in the treatment of central nervous system (CNS) disorders and AD [21,22].

Various syntheses of compounds containing bicyclo[3.2.1]octane/octene/octadiene cores are documented in the literature [23–27]. The benzobicyclo[3.2.1]octadiene skeleton can be constructed using different synthetic pathways, one of which is the photochemical approach that has been developed by our group in batch photochemical reactors [28–45]. Photochemically induced organic reactions provide an important and easy path to complex products from simple starting materials. The unsaturated bicyclo[3.2.1]octene structure can be even more useful than the saturated bicyclo[3.2.1]octane skeleton, as it can easily be transformed further by adding various functional groups to the isolated double bond. Our group obtained a whole library of complex polycyclic compounds with various functional groups by utilizing photochemical synthetic paths.

Compounds **1**–**14**, which were tested for cholinesterase inhibitory activity, make a core group selected from this vast library on the basis of preliminary basic in silico docking tests that were performed [35,41–43,45]. As far as the authors know, this is the first report on cholinesterase inhibitory activity using bicyclo[3.2.1]octadienes **1**–**11** and their (photo)transformation products **12**–**14** as potential inhibitors. Cedrol (**15**), a naturally occurring representative of these compounds, has also been tested for comparison. AChE/BChE inhibitory potential was also compared to standard AChE/BChE inhibitor huperzine A (hupA, **16**).

Antioxidant properties of these compounds (**1**–**15**) were investigated as a part of this study but were proven to be negligible and hence will not be discussed in great detail. The table with the results is given in the Supporting material (Table S1).

2. Results and discussion

Structures of tested bicyclo[3.2.1]octanes **1**–**14**, cedrol (**15**), and huperzine A (hupA, **16**) are given in Figure 1. The synthetic compounds are presented in small subgroups according to their structural similarities ending with naturally occurring compound cedrol (**15**) and standard AChE/BChE inhibitor hupA (**16**).

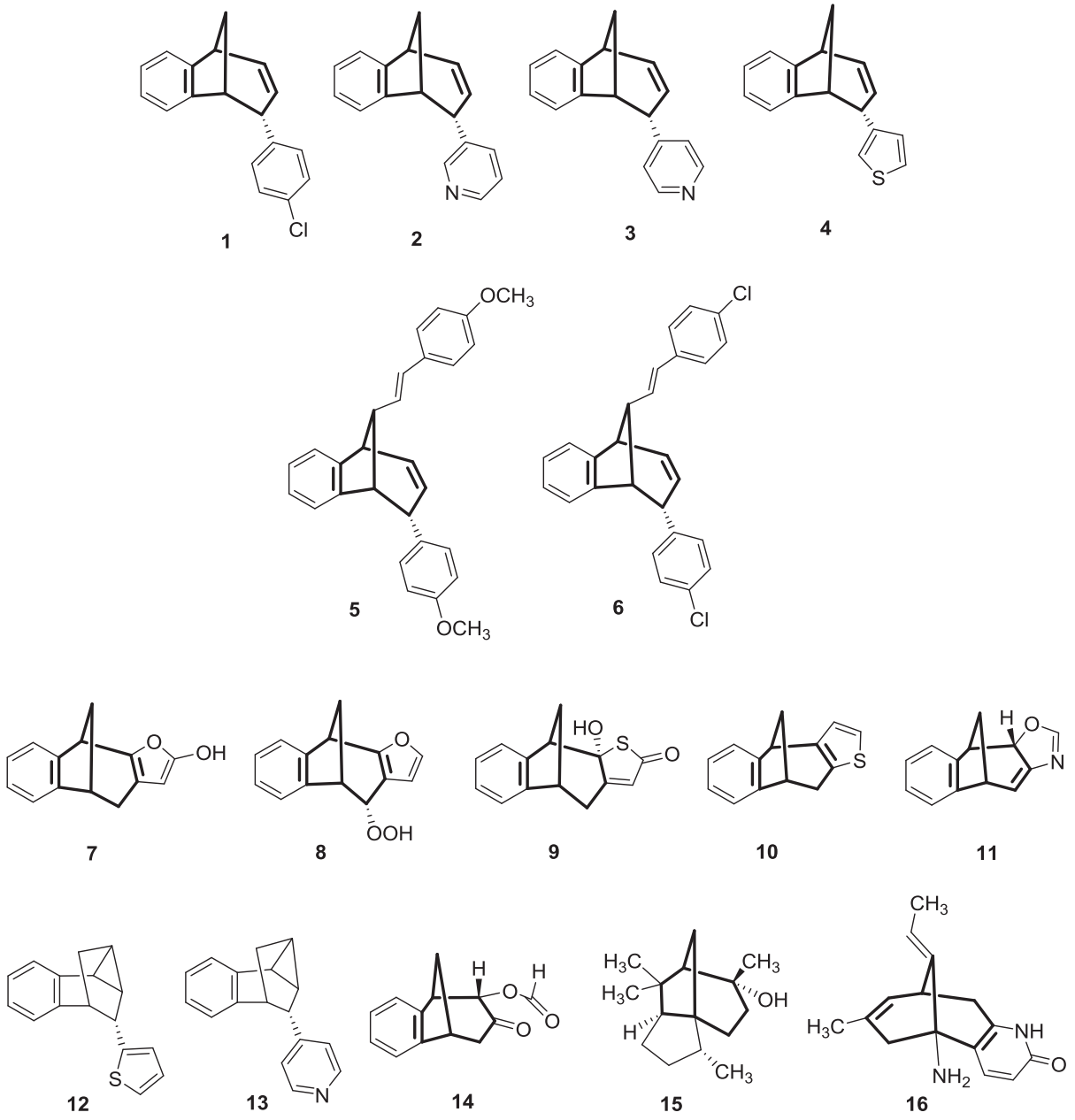

Figure 1. Structures of the tested polycyclic photoproducts **1**–**14**, the natural sesquiterpene alcohol cedrol (**15**), and alkaloid hupA (**16**).

To the best of our knowledge, the present paper reports the first investigation on ChE inhibitory activity of benzobicyclo[3.2.1]octadienes **1**–**11** and their (photo)transformation products **12**–**14**. AChE and BChE inhibitory activities were evaluated for 14 polycyclic photoproducts and a naturally occurring alcohol from

essential oils, cedrol (**15**), using the slightly modified Ellman method. The results are given in Table 1 and reported as IC_{50} values, where achieved, and as maximal inhibition at maximal concentration tested, where all concentrations are expressed in μM values. The calculated ADME characteristics of all 15 tested compounds are given in Table 2.

Table 1. Inhibitory activity of polycyclic photoproducts **1**–**14**, cedrol (**15**), and hupA (**16**) on two cholinesterases.

Compound	AChE		BChE	
	IC_{50} (μM)	Inhibition (%)[a]	IC_{50} (μM)	Inhibition (%)[a]
1	54.0	75.36 (127.8)	74.8	84.22 (127.8)
2	-	7.16 (204.5)	74.2	81.06 (204.5)
3	-	26.50 (23.1)	8.8	78.65 (23.1)
4	318.8	93.42 (954.5)	510.3	87.31 (954.5)
5	-	3.90 (9.6)	-	34.90 (9.6)
6	17.5	52.95 (18.8)	-	4.18 (18.8)
7	-	2.15 (428.2)	-	n.d. (428.2)
8	-	6.05 (398.2)	-	8.49 (398.2)
9	-	11.20 (405.5)	-	n.d. (405.5)
10	36.2	67.20 (53.5)	-	2.31 (53.5)
11	-	29.51 (691.4)	615.9	54.99 (691.4)
12	-	26.86 (19.1)	-	19.45 (19.1)
13	-	37.21 (350.9)	31.7	95.49 (350.9)
14	-	38.75 (1471.4)	335.7	77.83 (1471.4)
15	**-**	23.6 (218.7)	159.6	57.46 (218.7)
16	0.53	78.24 (1.88)	1350	60.73 (1875.8)

-, not determined; n.d., not detected; [a] numbers given in parentheses represent maximal concentrations tested in μM.

Among the 14 bicyclo[3.2.1]octenes/octadienes tested, all the compounds showed some inhibitory activity on both enzymes except for compounds **7** and **9**, which did not inhibit BChE at the concentrations tested.

Some compounds exhibited lower solubility in the final assay and therefore could not be tested at higher concentrations, i.e. **1**, **3**, **5**, **6**, **10**, **12**, **13**, and **15**. This was a limiting factor for the compounds **3**, **5**, and **12**, which showed potentially good inhibitory activity against AChE (26.50% at 23.1 μM), BChE (34.90% at 9.6 μM), and AChE (26.86% at 19.1 μM), respectively.

IC_{50} values were calculated for compounds **1**, **4**, **6**, and **10** for the AChE enzyme and compounds **1**–**4**, **11**, and **13**–**15** for the BChE enzyme.

The strongest inhibitor of AChE is compound **6**, having an IC_{50} value of 17.5 μM, while compound **3** showed the strongest inhibition of BChE, reaching an excellent IC_{50} value of 8.8 μM. Compounds **1** and **4** are the only compounds that inhibited both enzymes, reaching IC_{50} values of 54.0 and 318.8 μM (for AChE) and 74.8 and 510.3 μM (for BChE), respectively. It can be seen that these compounds showed stronger inhibitory activity against AChE than BChE and in both cases compound **1** showed up to six times stronger inhibitory activity.

When comparing compounds **1**–**6**, having the same benzobicyclo[3.2.1]octadiene core with different substituents, it can be concluded that the chlor-phenyl moiety (compounds **1** and **6**) seems to be favorable

Table 2. Calculated ADME properties of the tested polycyclic photoproducts **1**–**14** and the natural sesquiterpene alcohol cedrol (**15**).

Compound	LogP	Solubility [mg/mL]	Permeability [10^{-6} cm/s]	PPB [%]	CNS
1	5.53	0.001	195	98	–2.76
2	4.80	0.01	236	97	–2.50
3	4.12	0.03	244	95	–2.32
4	4.12	0.03	244	95	–2.32
5	2.58	0.03	237	76	–1.81
6	6.80	0.0003	37	99	–3.36
7	7.75	0.00001	5	100	–4.21
8	3.64	0.08	237	88	–2.02
9	3.20	0.03	234	85	–2.02
10	2.10	0.08	198	82	–2.15
11	4.42	0.01	242	92	–2.12
12	5.51	0.009	197	96	–2.41
13	4.55	0.02	240	96	–2.40
14	2.09	1.64	225	61	–1.76
15	5.05	0.19	198	77	–1.68

for AChE inhibitory activity. Compound **6**, a substituted analogue of compound **1**, exhibited three times stronger inhibitory activity (IC_{50} = 17.5 μM) and was the strongest inhibitor of the AChE enzyme among all of the tested compounds. This could be attributed to the "double" chlor-phenyl substitution in contrast to compound **1** (having only one). Also, compound **5** having "double" methoxy-phenyl substituents exhibited only negligible activity on AChE. On the other hand, compounds with pyridine moieties (**2** and **3**) are more favorable for BChE inhibition. The nitrogen position in the pyridine moiety represents a differentiating characteristic, making compound **3** almost nine times stronger an inhibitor of BChE than compound **2** and by far the strongest inhibitor of BChE among all of the polycycles tested.

Compounds **1**–**6** and **11**, which showed generally good inhibitory activity on both AChE and BChE, have two double bonds inside the 7-membered ring and a double bond inside the bicyclic ring, which was considered to be a favorable trait when evaluating ChE inhibition in earlier research [46,47].

When looking at the structures of compounds **7**–**11**, it can be seen that all of them have some type of heterocycle condensed to the basic benzobicyclo[3.2.1]octadiene core. Among this group of compounds, only compound **10**, having a tiophene ring condensed to the basic core, showed great inhibitory activity on AChE, with an IC_{50} of 36.2 μM. On the other hand, compound **11** exhibited relatively good inhibition of BChE, with an IC_{50} of 615.9 μM. Compounds **10** and **11** both have double bonds inside the polycyclic structure. All of the other compounds showed weak inhibitory activity for both of the enzymes (including **10** for BChE activity and **11** for AChE activity).

The phototransformation group of compounds **12**–**14** is structurally similar to previous compound subsets. Compound **13**, a phototransformation product of compound **3**, generally showed lower activity on both enzymes, although it had very good inhibitory activity for BChE with an IC_{50} of 31.7 μM. Figure 2 shows compounds **3** and **13** in a BChE active site.

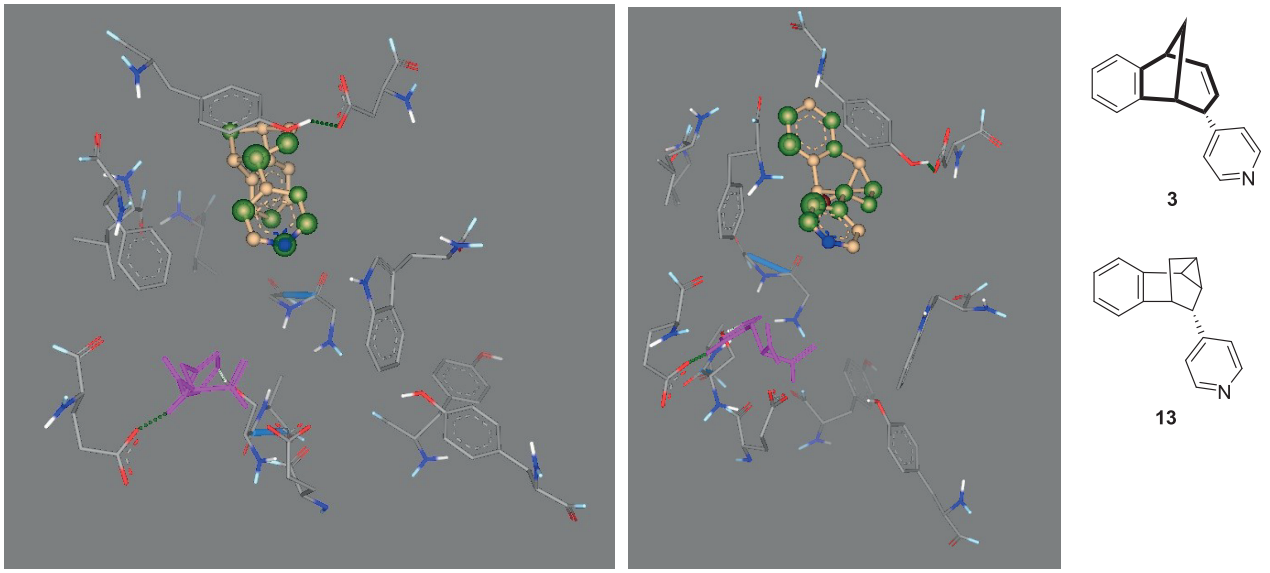

Figure 2. Compounds **3** (left) and **13** (right) at the active site of BChE (BChE-As). Member of the active site triad His 438 is given in pink.

Nevertheless, the activity was reduced by three times as a direct consequence of "tricycyclo" functionalization, which appears to have a negative effect on the inhibition of both enzymes.

Functionalized bicyclic compound **14** suits the inhibitory activity of BChE better than the closed ring as in **11** since it showed about one and a half times better activity, while compounds **7** and **8** showed only negligible BChE inhibitory activity.

Although compound **12** showed relatively weak activity among this subset of compounds, a closer reevaluation revealed that this compound showed potentially good inhibitory activity, showing about 20% inhibition at 19.1 μM on both enzymes, which we could not investigate further due to its solubility limits in the final assay.

Cedrol (**15**), as the only natural representative of bicyclo[3.2.1.]octanes, showed relatively weak activity on AChE and relatively good activity on BChE having an IC_{50} of 159.6 μM, making it the fifth best inhibitor among all compounds tested.

Huperzine A (hupA, **16**) is a known AChE/BChE inhibitor isolated from the Chinese medicinal herb *Huperzia serrata* (Thunb.) Trevis. with significantly high selectivity towards AChE [48–50] and with diverse inhibitory potential for BChE, depending on the source of the enzyme used [48,51,52]. When comparing the AChE inhibitory activity of the tested compounds (**1**–**15**) to hupA (**16**) it can be seen that compounds **6** and **1** are up to 30 and 100 times weaker inhibitors, respectively, which was expected due to high hupA selectivity for AChE. In the case of BChE inhibitory activity, hupA showed the weakest inhibitory potential of all compounds tested in this study, having an IC_{50} of 1350 μM. In comparison, the two strongest BChE inhibitors among the tested compounds, compounds **3** and **13**, showed 150 and 40 times stronger inhibitory activity.

In this study, the structure–property relationships [53–55] with predictive models (see Supporting material) for tested compounds **1**–**15** have been analyzed (Table 2). Physicochemical and ADME properties have been calculated, especially LogP, solubility, permeability across biological membranes, plasma protein binding (PPB), metabolic stability, and CNS penetration.

The ability to design drugs capable of penetrating the blood–brain barrier (BBB) and affecting the desired biological response is a formidable challenge. On the other hand, peripherally acting drugs need to possess specific physicochemical properties that prevent them from crossing the BBB. Fundamental physiochemical features of CNS drugs are related to their ability to penetrate the BBB affinity and exhibit CNS activity [54]. CNS drugs show characteristics of low molecular weight and lipophilicity and are hydrogen bond donors and acceptors that in general have a smaller range than general therapeutics.

As was mentioned before, some compounds having the same bicyclo[3.2.1]-core, as in the structures of **1**–**11**, **14**, and **15**, have proved to be potent inhibitors of dopamine and serotonin transporters and also play a crucial role in treatment of CNS disorders and AD [7]. Analyzing the obtained calculated values (Table 2), it is evident that almost all the compounds show significant CNS penetration properties, especially compounds **5**, **8**, **9**, **14**, and **15**.

Lipophilicity [53] was the first of the descriptors to be identified as important for CNS penetration. An analysis of small drug-like molecules suggested that for better brain penetration and for good intestinal permeability the LogP values need to be greater than 0 and less than 3. In silico analysis showed the best lipophilicity properties for structures **5**, **10**, and **14**, which means that they could possess good BBB penetration capability.

Commonly, the promising value of CNS penetration is higher than –3 and up to zero (see Table S2 in the Supporting material). Additionally, compounds **2**–**5**, **8**, **9**, **11**, **13**, and **14** have better PPB (Table 2) values than **1**, **6**, **7**, **10**, **12**, and **15**. Taking all ADME characteristics into account, it is evident that compound **14** has the best ADME properties among all of the compounds, although it showed inhibitory activity only towards BChE, and as such it could be a potential candidate for further research of BChE inhibition.

Preliminary docking experiments were performed with the SeeSAR software package (SeeSAR version 7.3; BioSolveIT GmbH, Sankt Augustin, Germany, 2018; www.biosolveit.de/SeeSAR). In silico experiments were done only for docking into the active sites of both AChE and BChE. From this it was seen that the software was unable to fit some of the molecules into the active pockets of AChE, those being **1**, **3**, **5**, **6**, and **11**. All of the other molecules could be placed into the active pockets with varied binding energies. We have given screenshots of all of the docking experiments performed in the supporting material (Figures S1–S12). In Figures 3 and 4, screenshots of compounds **1** and **4** docking into the active pockets of AChE and BChE are given. These ligands inhibited both enzymes, while compound **1** inhibited both enzymes six times more strongly than compound **4**.

When comparing the tested compounds to the study of Miyazawa and Yamafuji, who tested the AChE activity of 17 bicyclic monoterpenoid compounds, their achieved IC_{50} values were in range of 200 to 900 μM, while our compounds showed at least ten times stronger activity, falling into the range of 17.5–318.8 μM [46]. Another similar study by Gurjar et al. dealt with in silico studies and ChE inhibition characteristics of 22 imidazole analogues while trying to identify potential ChE inhibitors. In this study only ten analogues were identified having various degrees of activity towards either AChE or BChE, while only two were identified as most potent ones, reaching IC_{50} values of 5.33 μM for AChE and 4.99 μM for BChE, which represents results comparable to ours [56].

In conclusion, generally, more compounds inhibited BChE and achieved better IC_{50} values than those for AChE, the reason for which could be the fact that there are differences in the active site geometries and volumes of the two enzymes.

Compounds **3** and **6** showed the best inhibitory activity on BChE (IC_{50} = 8.8 μM) and AChE (IC_{50}

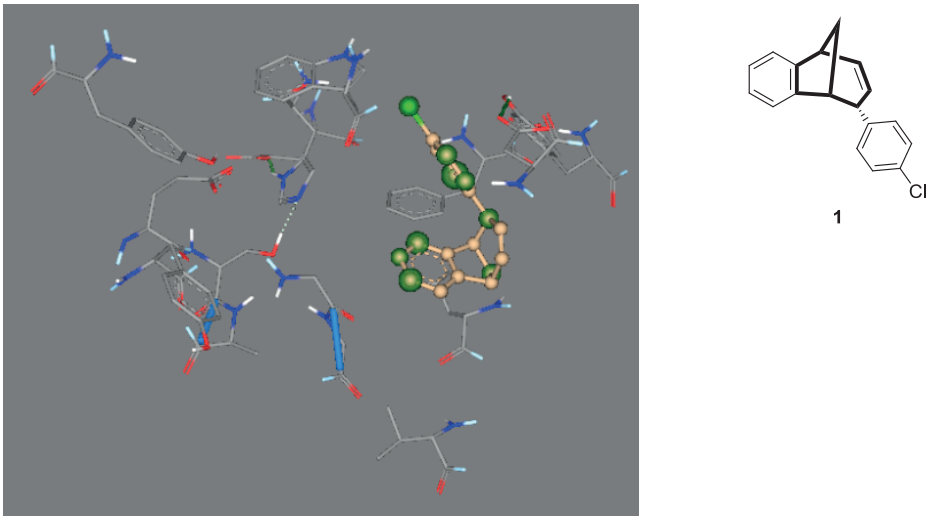

Figure 3. Compound **1** at the active site of BChE (BChE-As, left) with its structure given (right).

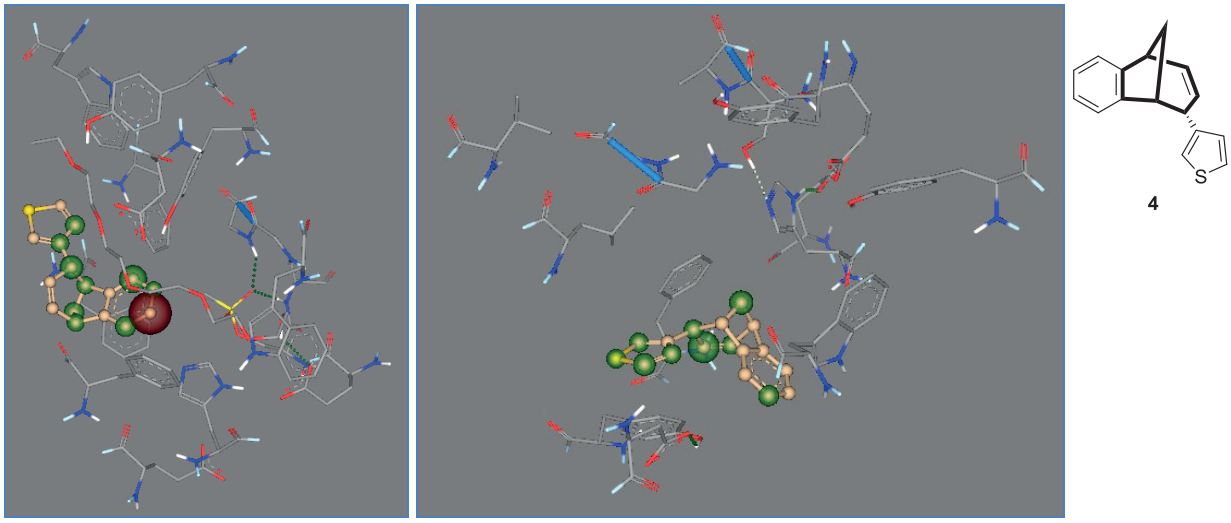

Figure 4. Compound **4** at the active site of AChE (AChE-As, left) and BCHE (BChE-As, right) with its structure given on the far right.

=1 7.5 μM), respectively, among all tested compounds. In comparison to hupA (**16**), compound **3** is about 150 times a better BChE inhibitor, while **6** is about 30 times weaker an AChE inhibitor, which also underlines the affinity of these compounds towards the BChE enzyme.

The structure–activity relationship principle reveals that pyridine substitution on the benzobicyclo[3.2.1]octadiene core is positively related to the BChE inhibitory strength and that the nitrogen position inside the pyridine ring plays an active role in BChE inhibition. Further cyclization of compounds with pyridine moiety, as in the case of **3**–**13**, seems to have a negative effect on the inhibition of both enzymes.

Chlor-phenyl substitution is positively related to the strength of AChE inhibition, especially when a "double" substitution occurs, while thiophene substitution of the benzobicyclo[3.2.1]octadiene core seems to decrease the inhibitory activity of both enzymes.

Bearing in mind that a single inhibitor capable of inhibiting both AChE and BChE would be preferable in the case of AD treatment, compounds **1** and **4** represent good starting points in the further development of ChE inhibitors.

3. Experimental

All reagents and solvents used were of analytical grade. Acetylcholinesterase (AChE, from *Electrophorus electricus* – electric eel, type V-S, C2888), butyrylcholinesterase (BChE, from equine serum, C7512), acetylthiocholine iodide (ATChI), butyrylthiocholine iodide (BTChI), 5,5-dithiobis (2-nitrobenzoic acid) (DTNB, Ellman's reagent), (1*S*, 2*R*, 5*S*, 7*R*, 8*R*)-2,6,6,8-tetramethyltricyclo[5.3.1.0^{1,5}]undecan-8-ol (cedrol, **15**), and (1*R*,9*R*,13*E*)-1-amino-13-ethylidene-11-methyl-6-azatricyclo[7.3.1.0^{2,7}]trideca-2(7),3,10-trien-5-one (huperzine A, **16**) were purchased from Sigma-Aldrich GmbH (Steinheim, Germany). Absorbance measurements were performed using a Synergy HTX S1LFA multimode microplate reader (BioTek Instruments, Inc., Winooski, VT, USA). All the tested polycyclic derivatives, (11*S*)-11-(4-chlorophenyl)tricyclo[6.3.1.0^{2,7}]dodeca-2,4,6,9-tetraene (**1**), 3-[(9*S*)-tricyclo[6.3.1.0^{2,7}]dodeca-2,4,6,10-tetraen-9-yl]pyridine (**2**), 4-[(9*S*)-tricyclo[6.3.1.0^{2,7}]dodeca-2,4,6,10-tetraen-9-yl]pyridine (**3**), 3-[(9*S*)-tricyclo[6.3.1.0^{2,7}]dodeca-2(7),3,5,10-tetraen-9-yl]thiophene (**4**), (11*S*)-11-(4-methoxyphenyl)-12-[(*E*)-2-(4-methoxyphenyl)ethenyl]tricyclo[6.3.1.0^{2,7}]dodeca-2,4,6,9-tetraene (**5**), (11*S*)-11-(4-chlorophenyl)-12-[(*E*)-2-(4-chlorophenyl)ethenyl]tricyclo[6.3.1.0^{2,7}]dodeca-2,4,6,9-tetraene (**6**), 3-oxatetracyc-lo[6.6.1.0^{2,6}.0^{9,14}]pentadeca-2(6),4,9(14),10,12-pentaen-4-ol (**7**), 3-oxatetracyclo[6.6.1.0^{2,6}.0^{9,14}]pentadeca-2(6),4,9(14),10,12-pentaene-7-peroxol (**8**), 2-hydroxy-3-thiatetracyclo[6.6.1.0^{2,6}.0^{9,14}]pentadeca-5,9(14),10,12-tetraen-4-one (**9**), 5-thiatetracyclo[6.6.1.0^{2,6}.0^{9,14}]pentadeca-2(6),3,9(14),10,12-pentaene (**10**), (2*S*)-3-oxa-5-azatetracyclo[6.6.1.0^{2,6}.0^{9,14}]pentadeca-4,6,9,11,13-pentaene (**11**), 2-[(10*S*)-tetracyclo[7.2.1.0^{2,11}.0^{3,8}]dodeca-3(8),4,6-trien-10-yl]thiophene (**12**), 4-[(10*S*)-tetracyclo[7.2.1.0^{2,11}.0^{3,8}]dodeca-3,5,7-trien-10-yl]pyridine (**13**), and (9*S*)-10-oxotricyclo[6.3.1.0^{2,7}]dodeca-2,4,6-trien-9-yl formate (**14**), were prepared as described previously [35,41–43,45].

3.1. Acetylcholinesterase/butyrylcholinesterase inhibitory activity

AChE/BChE inhibitory activity measurements were carried out by a slightly modified Ellman assay as described before [57]. The results are expressed as percentage inhibition of enzyme activity or IC_{50}.

3.2. In silico docking experiments

Docking experiments were performed in silico with the SeeSAR package (SeeSAR version 7.3; BioSolveIT GmbH, Sankt Augustin, Germany, 2018; www.biosolveit.de/SeeSAR). Docking was performed for the active site of the acetylcholinesterase (AChE-As extracted from 4M0E) and the active site of the butyrylcholinesterase (BChE-As extracted from 1P0I) [11,58]. The software could not fit some of the molecules (**1**, **4**–**7**) into the active pockets of the acetylcholinesterase, but for all of the other ligands that were tested screenshots of the best docking hits are given in the Supporting material (Figures S1–S12).

3.3. ADME characteristics determination

ADME characteristics for tested compounds **1**–**14** and cedrol (**15**) were predicted by Pass (in silico) software [http://www.way2drug.com/PASSOnline/]. An explanation of all parameters evaluated is given in Table S2 in the Supporting material.

Acknowledgment

This research was fully supported by the Croatian Science Foundation under Project IP-09-2014-6897, "Investigation of bioactive compounds from Dalmatian plants: their antioxidant, enzyme inhibition, and health properties".

Author contributions

F. Burčul and I. Škorić designed the study and planned the paper and equally contributed to it. Biological testing was designed and performed by F. Burčul. I. Šagud, D. Vuk, and A. Ratković synthesized the bicyclo[3.2.1]octenes and bicyclo[3.2.1]octadienes. All the authors analyzed the data and helped finalize the manuscript.

References

1. Kukull WA, Higdon R, Bowen JD, McCormick WC, Teri L et al. Dementia and Alzheimer disease incidence: a prospective cohort study. Archives of Neurology 2002; 59 (11): 1737-1746. doi: 10.1001/archneur.59.11.1737
2. Tarawneh R. Holtzman DM. The clinical problem of symptomatic alzheimer disease and mild cognitive impairment. Cold Spring Harbor Perspectives in Medicine 2012; 2 (5): 1-16. doi: 10.1101/cshperspect.a006148
3. Khan MTH. Molecular interactions of cholinesterases inhibitors using in silico methods: current status and future prospects. New Biotechnology 2009; 25 (5): 331-346. doi: https://doi.org/10.1016/j.nbt.2009.03.008
4. Masson P, Carletti E, Nachon F. Structure, activities and biomedical applications of human butyrylcholinesterase. Protein and Peptide Letters 2009; 16 (10): 1215-1224. doi: http://dx.doi.org/10.2174/092986609789071207
5. Öztaskın N, Taslimi P, Maraş A, Gülcin İ. Göksu S. Novel antioxidant bromophenols with acetylcholinesterase, butyrylcholinesterase and carbonic anhydrase inhibitory actions. Bioorganic Chemistry 2017; 74: 104-114. doi: https://doi.org/10.1016/j.bioorg.2017.07.010
6. Akıncıoğlu A, Kocaman E, Akıncıoğlu H, Salmas RE, Durdagi S et al. The synthesis of novel sulfamides derived from β-benzylphenethylamines as acetylcholinesterase, butyrylcholinesterase and carbonic anhydrase enzymes inhibitors. Bioorganic Chemistry 2017; 74: 238-250. doi: https://doi.org/10.1016/j.bioorg.2017.08.012
7. Burčul F, Radan M, Politeo O. Blažević I. Cholinesterase-inhibitory activity of essential oils. In: Taylor JC (editor). Advances in Chemistry Research. New York, NY, USA: Nova Science Publishers Inc., 2017, pp. 1-71.
8. Gulçin İ, Abbasova M, Taslimi P, Huyut Z, Safarova L et al. Synthesis and biological evaluation of aminomethyl and alkoxymethyl derivatives as carbonic anhydrase, acetylcholinesterase and butyrylcholinesterase inhibitors. Journal of Enzyme Inhibition and Medicinal Chemistry 2017; 32 (1): 1174-1182. doi: 10.1080/14756366.2017.1368019
9. Greig NH, Utsuki T, Ingram DK, Wang Y, Pepeu G et al. Selective butyrylcholinesterase inhibition elevates brain acetylcholine, augments learning and lowers Alzheimer β-amyloid peptide in rodent. Proceedings of the National Academy of Sciences of the United States of America 2005; 102 (47): 17213-17218. doi: 10.1073/pnas.0508575102
10. Giacobini E. Cholinesterase inhibitors: new roles and therapeutic alternatives. Pharmacological Research 2004; 50 (4): 433-440. doi: https://doi.org/10.1016/j.phrs.2003.11.017
11. Nicolet Y, Lockridge O, Masson P, Fontecilla-Camps JC, Nachon F. Crystal structure of human butyrylcholinesterase and of its complexes with substrate and products. Journal of Biological Chemistry 2003; 278 (42): 41141-41147. doi: 10.1074/jbc.M210241200
12. Dvir H, Silman I, Harel M, Rosenberry TL. Sussman JL. Acetylcholinesterase: from 3D structure to function. Chemico-Biological Interactions 2010; 187 (1): 10-22. doi: https://doi.org/10.1016/j.cbi.2010.01.042

13. Abad A, Agulló C, Cuñat A, De Alfonso I, Navarro I et al. Synthesis of highly functionalised enantiopure bicyclo[3.2.1]-octane systems from carvone. Molecules 2004; 9 (5): 287-299.

14. Miller JA, Harris J, Miller AA, Ullah GM, Welsh GM. Synthesis of 8-substituted bicyclo[3.2.1]octane-6-carboxylic acids and anti-convulsant properties of the corresponding amides. Tetrahedron Letters 2004; 45 (22): 4323-4327. doi: https://doi.org/10.1016/j.tetlet.2004.04.007

15. Thomson CG, Carlson E, Chicchi GG, Kulagowski JJ, Kurtz MM et al. Synthesis and structure–activity relationships of 8-azabicyclo[3.2.1]octane benzylamine NK1 antagonists. Bioorganic & Medicinal Chemistry Letters 2006; 16 (4): 811-814. doi: https://doi.org/10.1016/j.bmcl.2005.11.026

16. Mascitti V. Préville C. Stereoselective synthesis of a dioxa-bicyclo[3.2.1]octane SGLT2 inhibitor. Organic Letters 2010; 12 (13): 2940-2943. doi: 10.1021/ol100940w

17. Kavitha CV, Nambiar M, Narayanaswamy PB, Thomas E, Rathore U et al. Propyl-2-(8-(3,4-difluorobenzyl)-2′,5′-dioxo-8-azaspiro[bicyclo[3.2.1] octane-3,4′-imidazolidine]-1′-yl) acetate induces apoptosis in human leukemia cells through mitochondrial pathway following cell cycle arrest. PLoS One 2013; 8 (7): e69103. doi: 10.1371/journal.pone.0069103

18. Kraus GA, Hon YS, Sy J. Synthesis of bicyclo[3.2.1]octanes by ring contraction. Journal of Organic Chemistry 1986; 51 (14): 2625-2627. doi: 10.1021/jo00364a001

19. Filippini MH, Rodriguez J. Synthesis of functionalized bicyclo[3.2.1]octanes and their multiple uses in organic chemistry. Chemical Reviews 1999; 99 (1): 27-76. doi: 10.1021/cr970029u

20. Presset M, Coquerel Y, Rodriguez J. Syntheses and applications of functionalized bicyclo[3.2.1]octanes: thirteen years of progress. Chemical Reviews 2013; 113 (1): 525-595. doi: 10.1021/cr200364p

21. Meltzer PC, Blundell P, Yong YF, Chen Z, George C et al. 2-Carbomethoxy-3-aryl-8-bicyclo[3.2.1]octanes: potent non-nitrogen inhibitors of monoamine transporters. Journal of Medicinal Chemistry 2000; 43 (16): 2982-2991. doi: 10.1021/jm000191g

22. Mandzhulo AY, Mel'nichuk NA, Fetyukhin VN, Vovk MV. Synthesis of 4′-alkyl-8-azaspiro[bicyclo[3.2.1]octane-3,2′-morpholin]-5′-ones. Russian Journal of Organic Chemistry 2016; 52 (1): 87-91. doi: 10.1134/S1070428016010164

23. Klumpp GW, Barnick JWFK, Veefkind AH, Bickelhaupt F. The synthesis of substituted bicyclo[3.2.1]octa-2,6-dienes. Recueil des Travaux Chimiques des Pays-Bas 1969; 88 (7): 766-778. doi: doi:10.1002/recl.19690880702

24. Nitta M, Okada S, Kato M. Stereoelectronic and homoconjugative effect of stereoselectivity. The addition of dichlorocarbene to 1,5-dimethyl-6-methylenetricyclo[3.2.1.02,7]oct-3-en-8-one and its related compounds. Bulletin of the Chemical Society of Japan 1984; 57 (9): 2463-2467. doi: 10.1246/bcsj.57.2463

25. Jones PS, Smith PW, Hardy GW, Howes PD, Upton RJ et al. Synthesis of tetrasubstituted bicyclo[3.2.1]octenes as potential inhibitors of influenza virus sialidase. Bioorganic and Medicinal Chemistry Letters 1999; 9 (4): 605-610. doi: https://doi.org/10.1016/S0960-894X(99)00032-3

26. Sakata J, Ando Y, Ohmori K, Suzuki K. Synthetic study on naphthospironone A: construction of benzobicyclo[3.2.1]octene skeleton with oxaspirocycle. Organic Letters 2015; 17 (15): 3746-3749. doi: 10.1021/acs.orglett.5b01732

27. Su X, Sun Y, Yao J, Chen H, Chen C. Acid-promoted bicyclization of arylacetylenes to benzobicyclo[3.2.1]octanes through cationic rearrangements. Chemical Communications 2016; 52 (24): 4537-4540. doi: 10.1039/C6CC00452K

28. Šindler-Kulyk M, Špoljarić L, Marinić Ž. Photochemistry of β-(2-furyl) substituted o-divinylbenzenes. Heterocycles 1989; 29 (4): 679-682. doi: 10.3987/COM-89-4629

29. Šindler-Kulyk M, Tomšić S, Marinić Ž, Metelko B. Synthesis and photochemistry of 2-styrylpyrroles. Intermolecular photoaddition of pyrroles to a double bond. Recueil des Travaux Chimiques des Pays-Bas 1995; 114 (11-12): 476-479. doi: doi:10.1002/recl.19951141109

30. Sindler-Kulyk M, Skoric I, Tomsic S, Marinic Z, Mrvos-Sermek D. Synthesis and photochemistry of styryl substituted annelated furan derivatives. Heterocycles 1999; 51 (6): 1355-1369. doi: 10.3987/COM-99-8502

31. Škorić I, Basarić N, Marinić Z, Šindler-Kulyk M. Observation of the primary intermediates in the photochemistry of o-vinylstyrylfurans. Heterocycles 2001; 55 (10): 1889-1896. doi: 10.3987/COM-01-9314

32. Basarić N, Marinić Ž, Šindler-Kulyk M. Photochemical formation of novel pyrrolo[3,2-b]-6,7-benzobicyclo[3.2.1]octa-2,6-diene. Journal of Organic Chemistry 2003; 68 (19): 7524-7527. doi: 10.1021/jo0346454

33. Škorić I, Basarić N, Marinić Ž, Višnjevac A, Kojić-Prodić B et al. Synthesis and photochemistry of β,β'-di(2-furyl)-substituted o-divinylbenzenes: intra- and/or intermolecular cycloaddition as an effect of annelation. Chemistry-A European Journal 2005; 11 (2): 543-551. doi: doi:10.1002/chem.200401005

34. Škorić I, Flegar I, Marinić Ž, Šindler-Kulyk M. Synthesis of the novel conjugated ω,ω'-diaryl/heteroaryl hexatriene system with the central double bond in a heteroaromatic ring: photochemical transformations of 2,3-divinylfuran derivatives. Tetrahedron 2006; 62 (31): 7396-7407. doi: https://doi.org/10.1016/j.tet.2006.05.034

35. Vidaković D, Škorić I, Horvat M, Marinić Ž, Šindler-Kulyk M. Photobehaviour of 2- and 3-heteroaryl substituted o-divinylbenzenes; formation of fused 2,3- and 3,2-heteroareno-benzobicyclo[3.2.1]octadienes and 3-heteroaryl benzobicyclo[2.1.1]hexenes. Tetrahedron 2008; 64 (18): 3928-3934. doi: https://doi.org/10.1016/j.tet.2008.02.062

36. Škorić I, Šmehil M, Marinić Ž, Molčanov K, Kojić-Prodić B et al. Photochemistry of ω-(o-vinylphenyl)-ω'-(phenyl/2-furyl) butadienes: new approach to 4-substituted benzobicyclo[3.2.1]octadienes. Journal of Photochemistry and Photobiology A: Chemistry 2009; 207 (2): 190-196. doi: https://doi.org/10.1016/j.jphotochem.2009.07.008

37. Kikaš I, Škorić I, Marinić Ž, Šindler-Kulyk M. Synthesis and phototransformations of novel styryl-substituted furo-benzobicyclo[3.2.1]octadiene derivatives. Tetrahedron 2010; 66 (48): 9405-9414. doi: https://doi.org/10.1016/j.tet.2010.09.093

38. Kikaš I, Horváth O, Škorić I. Functionalization of the benzobicyclo[3.2.1]octadiene skeleton via photocatalytic and thermal oxygenation of a furan derivative. Tetrahedron Letters 2011; 52 (47): 6255-6259. doi: https://doi.org/10.1016/j.tetlet.2011.09.076

39. Škorić I, Kikaš I, Kovács M, Fodor L, Marinić Ž et al. Synthesis, photochemistry, and photophysics of butadiene derivatives: influence of the methyl group on the molecular structure and photoinduced behavior. Journal of Organic Chemistry 2011; 76 (21): 8641-8657. doi: 10.1021/jo200691x

40. Kikaš I, Horváth O, Škorić I. Functionalization of the benzobicyclo[3.2.1]octadiene skeleton via photocatalytic oxygenation of furan and benzofuran derivatives. Journal of Molecular Structure 2013; 1034: 62-68. doi: https://doi.org/10.1016/j.molstruc.2012.09.005

41. Vuk D, Potroško D, Šindler-Kulyk M, Marinić Ž, Molčanov K et al. Synthesis and photochemical transformations of new butadiene chromophores: the influence of the nature and position of chlorine substituent on the photoinduced behaviour. Journal of Molecular Structure 2013; 1051: 1-14. doi: https://doi.org/10.1016/j.molstruc.2013.07.052

42. Vuk D, Kikaš I, Molčanov K, Horváth O, Škorić I. Functionalization of the benzobicyclo[3.2.1]octadiene skeleton via photocatalytic oxygenation of thiophene and furan derivatives: the impact of the type and position of the heteroatom. Journal of Molecular Structure 2014; 1063: 83-91. doi: https://doi.org/10.1016/j.molstruc.2014.01.055

43. Vuk D, Marinić Ž. Škorić I. Photochemical approach to new polycyclic substrates suitable for further photocatalytic functionalization. Croatica Chemica Acta 2014; 87 (4): 465-473. doi: 10.5562/cca2454

44. Vuk D, Horváth O, Marinić Ž, Škorić I. Functionalization of the benzobicyclo[3.2.1] octadiene skeleton possessing one isolated double bond via photocatalytic oxygenation. Journal of Molecular Structure 2016; 1107: 70-76. doi: https://doi.org/10.1016/j.molstruc.2015.11.036

45. Šagud I, Levačić M, Marinić Ž, Škorić I. Formation of polycyclic skeletons by photochemical transformations of pyridyl- and thienylbutadiene derivatives. European Journal of Organic Chemistry 2017; 2017 (26): 3787-3794. doi: doi:10.1002/ejoc.201700481

46. Miyazawa M, Yamafuji C. Inhibition of acetylcholinesterase activity by bicyclic monoterpenoids. Journal of Agricultural and Food Chemistry 2005; 53 (5): 1765-1768. doi: 10.1021/jf040019b

47. Greenblatt HM, Kryger G, Lewis T, Silman I, Sussman JL. Structure of acetylcholinesterase complexed with (–)-galanthamine at 2.3 Å resolution. FEBS Letters 1999; 463 (3): 321-326. doi: doi:10.1016/S0014-5793(99)01637-3

48. Bai D. Development of huperzine A and B for treatment of Alzheimer's disease. Pure and Applied Chemistry 2007; 79 (4): 469-479. doi: 10.1351/pac200779040469

49. Haigh JR, Johnston SR, Peppernay A, Mattern PJ, Garcia GE et al. Protection of red blood cell acetylcholinesterase by oral huperzine A against ex vivo soman exposure: next generation prophylaxis and sequestering of acetylcholinesterase over butyrylcholinesterase. Chemico-Biological Interactions 2008; 175 (1): 380-386. doi: https://doi.org/10.1016/j.cbi.2008.04.033

50. Lockridge O. Review of human butyrylcholinesterase structure, function, genetic variants, history of use in the clinic, and potential therapeutic uses. Pharmacology and Therapeutics 2015; 148: 34-46. doi: https://doi.org/10.1016/j.pharmthera.2014.11.011

51. Tang XC, Han YF. Pharmacological profile of huperzine A, a novel acetylcholinesterase inhibitor from Chinese herb. CNS Drug Reviews 1999; 5 (3): 281-300. doi: 10.1111/j.1527-3458.1999.tb00105.x

52. Wang R, Yan H, Tang XC. Progress in studies of huperzine A, a natural cholinesterase inhibitor from Chinese herbal medicine. Acta Pharmacologica Sinica 2006; 27: 1-26. doi: 10.1111/j.1745-7254.2006.00255.x

53. Testa B, Crivori P, Reist M, Carrupt PA. The influence of lipophilicity on the pharmacokinetic behavior of drugs: concepts and examples. Perspectives in Drug Discovery and Design 2000; 19 (1): 179-211. doi: 10.1023/a:1008741731244

54. Alavijeh MS, Chishty M, Qaiser MZ, Palmer AM. Drug metabolism and pharmacokinetics, the blood-brain barrier, and central nervous system drug discovery. NeuroRx 2005; 2 (4): 554-571. doi: 10.1602/neurorx.2.4.554

55. Pajouhesh H, Lenz GR. Medicinal chemical properties of successful central nervous system drugs. NeuroRx 2005; 2 (4): 541-553. doi: 10.1602/neurorx.2.4.541

56. Gurjar AS, Darekar MN, Yeong KY, Ooi L. In silico studies, synthesis and pharmacological evaluation to explore multi-targeted approach for imidazole analogues as potential cholinesterase inhibitors with neuroprotective role for Alzheimer's disease. Bioorganic & Medicinal Chemistry 2018; 26 (8): 1511-1522. doi: https://doi.org/10.1016/j.bmc.2018.01.029

57. Burčul F, Generalić Mekinić I, Radan M, Rollin P, Blažević I. Isothiocyanates: cholinesterase inhibiting, antioxidant, and anti-inflammatory activity. Journal of Enzyme Inhibition and Medicinal Chemistry 2018; 33 (1): 577-582. doi: 10.1080/14756366.2018.1442832

58. Cheung J, Gary EN, Shiomi K, Rosenberry TL. Structures of human acetylcholinesterase bound to dihydrotanshinone I and territrem B show peripheral site flexibility. ACS Medicinal Chemistry Letters 2013; 4 (11): 1091-1096. doi: 10.1021/ml400304w

Supplementary materials

Docking experiments were performed in silico with the SeeSAR package, version 7.3 (BioSolveIT GmbH, Sankt Augustin, Germany, 2018; www.biosolveit.de/SeeSAR). Experiments were performed for the active sites of acetylcholinesterase (AChE-As) and butyrylcholinesterase (BChE-As). The software could not fit some of the molecules (**1**, **4**–**7**) into the active site of acetylcholinesterase. Screenshots of the best docking hits are given below for all compounds tested. Green haloes show places of bonding (negative binding energies, energy released) and red ones show places of antibonding.

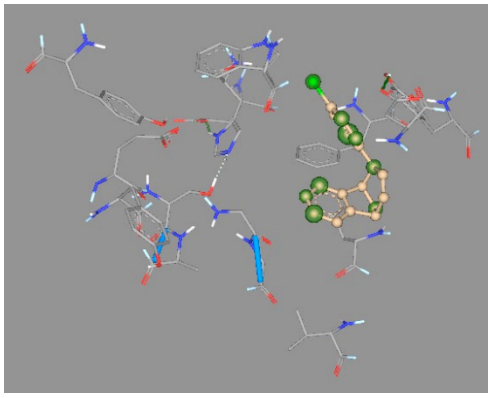

Figure S1. Compound **1** at the active site of butyrylcholinesterase (BChE-As).

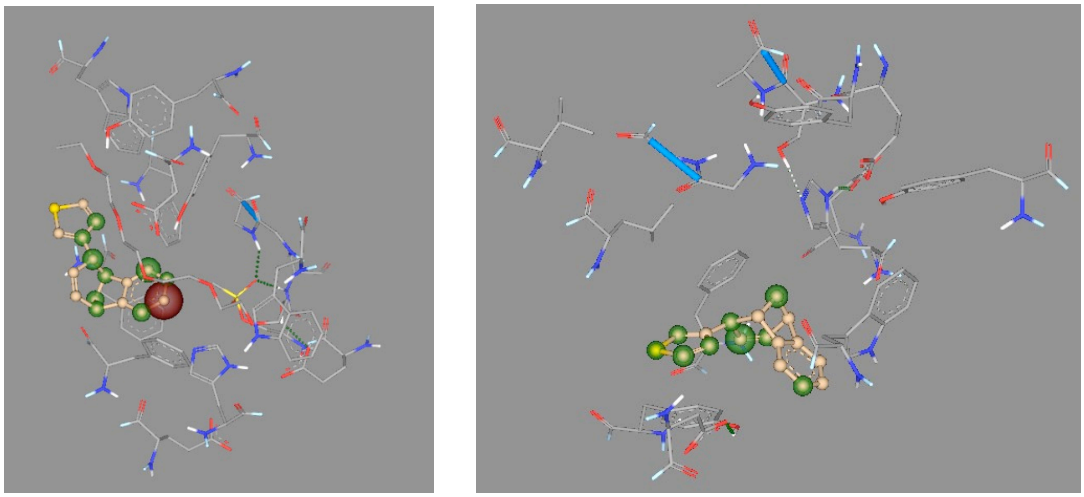

Figure S2. Compound **2** at the active site of acetylcholinesterase (AChE-As, left) and butyrylcholinesterase (BChE-As, right).

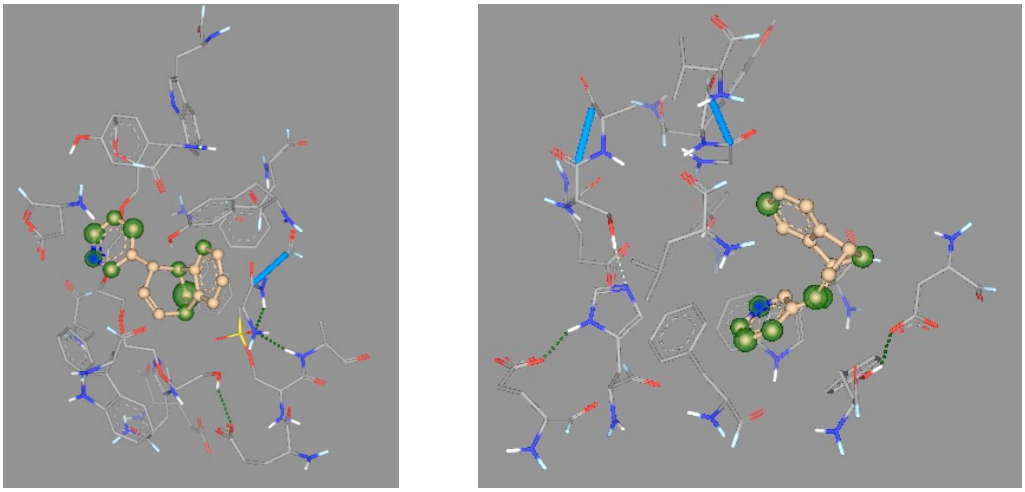

Figure S3. Compound **3** at the active site of AChE-As (left) and BChE-As (right).

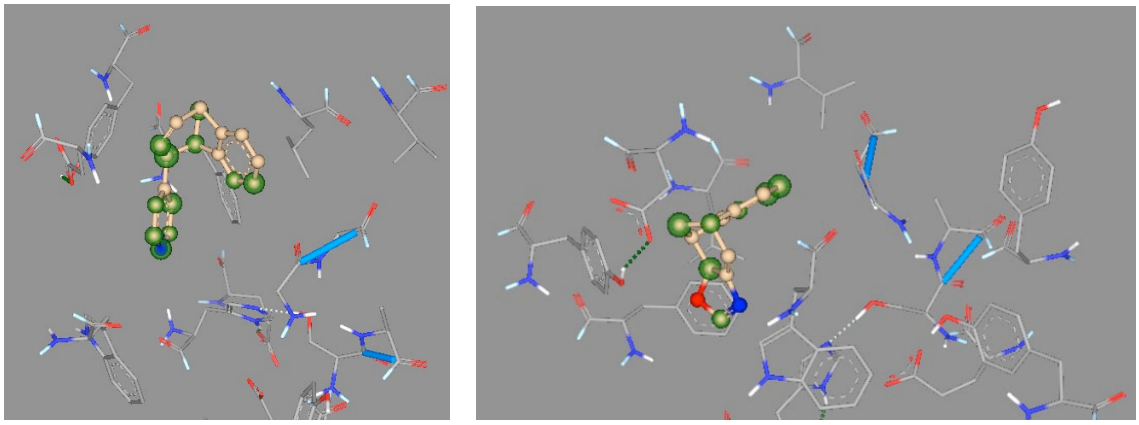

Figure S4. Compounds **4** (left) and **5** (right) at the active site of BChE-As.

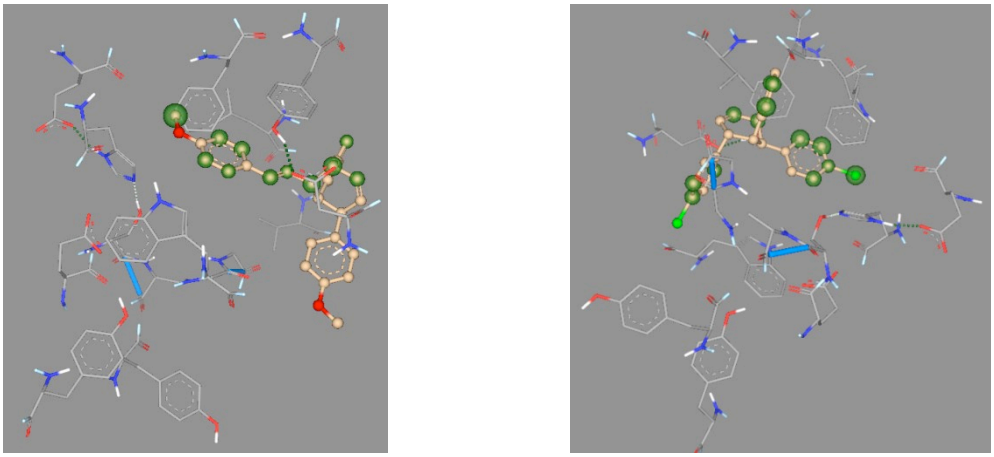

Figure S5. Compounds **6** (left) and **7** (right) at the active site of BChE-As.

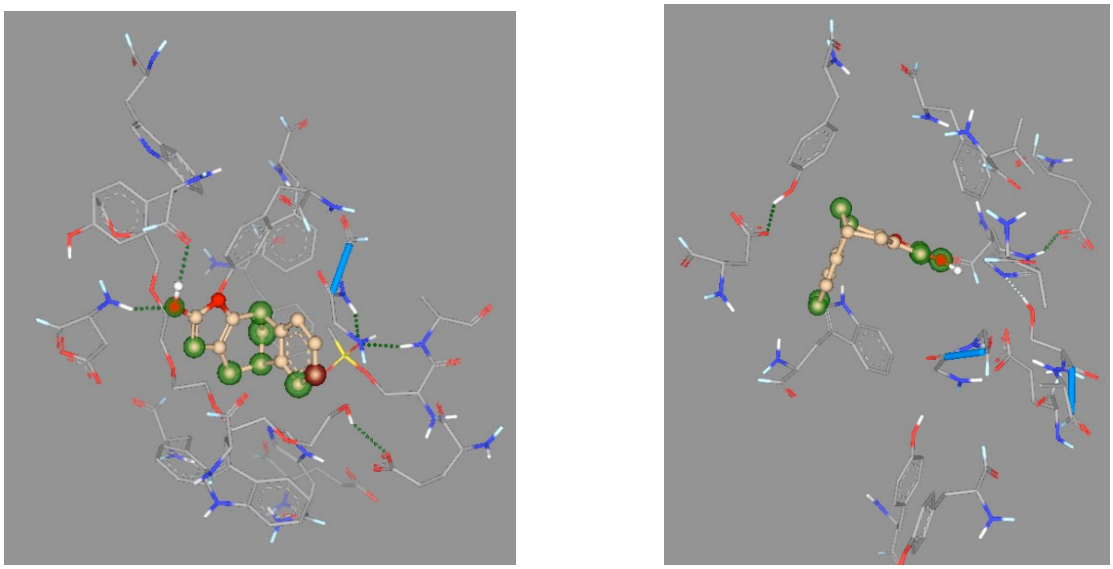

Figure S6. Compound **8** at the active site of AChE-As (left) and BChE-As (right).

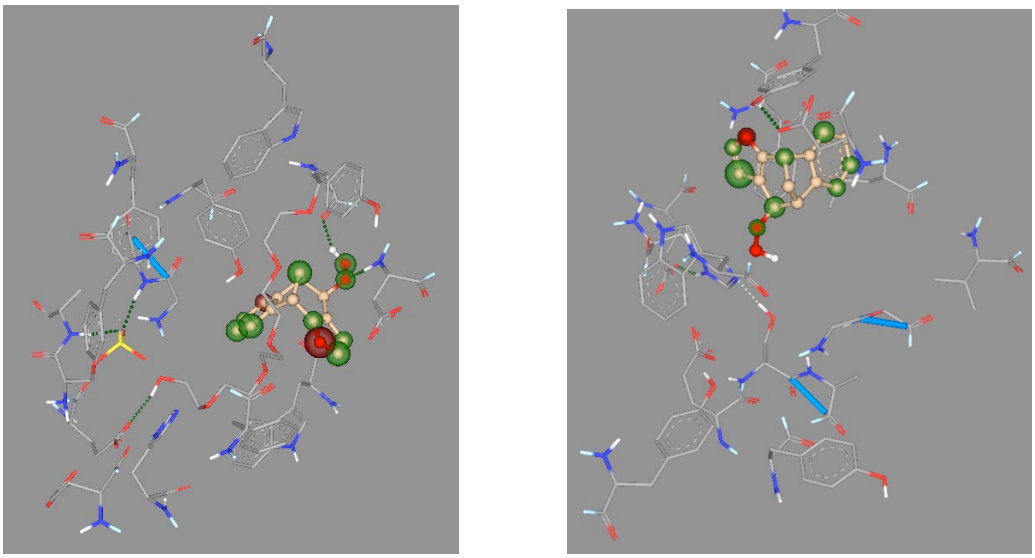

Figure S7. Compound **9** at the active site of AChE-As (left) and BChE-As (right).

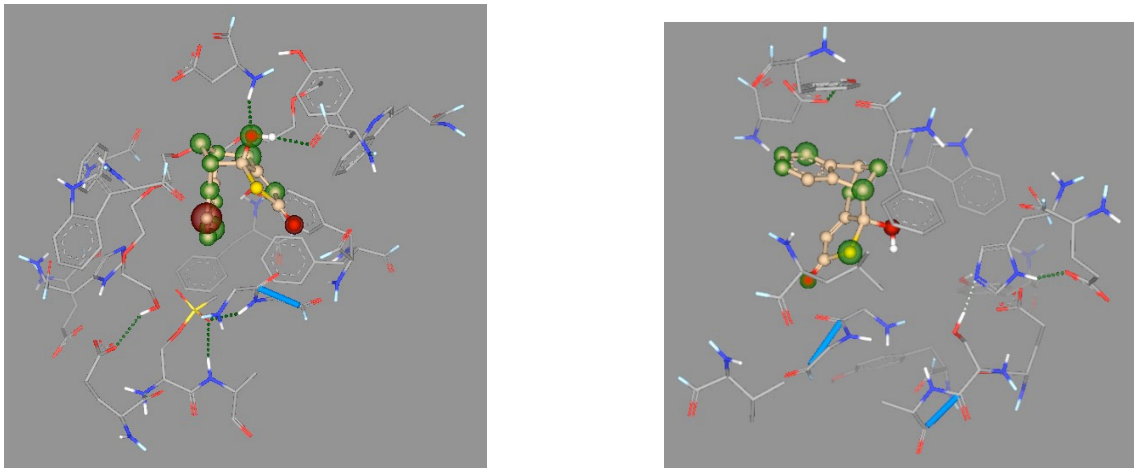

Figure S8. Compound **10** at the active site of AChE-As (left) and BChE-As (right).

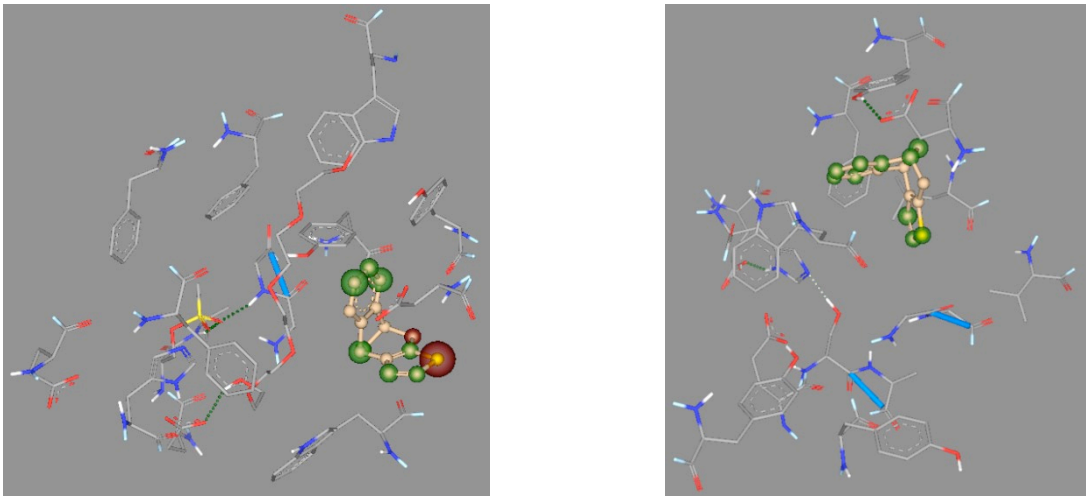

Figure S9. Compound **11** at the active site of AChE-As (left) and BChE-As (right).

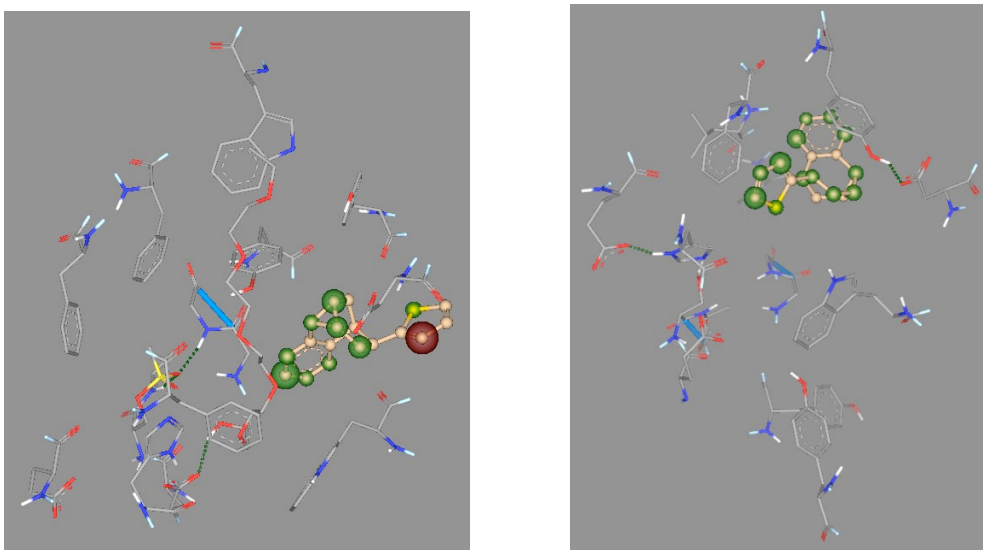

Figure S10. Compound **12** at the active site of AChE-As (left) and BChE-As (right).

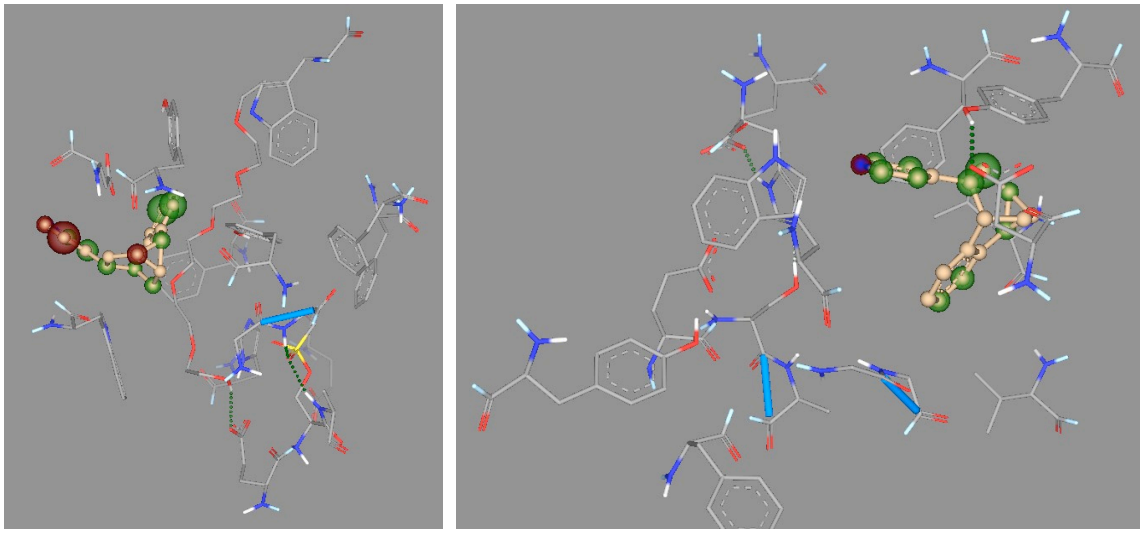

Figure S11. Compound **13** at the active site of AChE-As (left) and BChE-As (right).

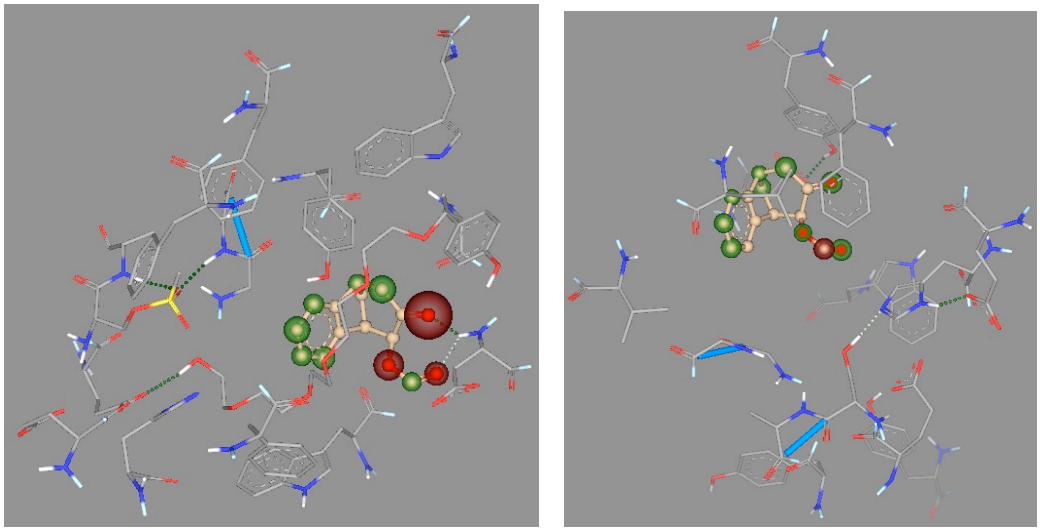

Figure S12. Compound **14** at the active site of AChE-As (left) and BChE-As (right).

Antioxidant properties of these compounds were also tested as a part of this study but were proven to be negligible. The table with the results is given below.

Table S1. Antioxidant properties of polycyclic photoproducts **1**–**14** and cedrol (**15**) using DPPH and FRAP methods.

Polycycle	DPPH	FRAP
	Inhibition % [a]	Equiv. Fe^{2+} μM [b]
1	n.d. (at 540)	n.d. (at 8.8)
2	9.18 (at 210)	n.d. (at 150)
3	45.51 (at 390)	n.d. (at 260)
4	0.87 (at 1000)	322.44 (at 680)
5	17.90 (at 160)	n.d. (at 6.88)
6	n.d. (at 160)	n.d. (at 13.75)
7	0.86 (at 450)	n.d. (at 300)
8	5.06 (at 420)	n.d. (at 280)
9	n.d. (at 420)	n.d. (at 290)
10	2.15 (at 1520)	1233.06 (at 1520)
11	1.68 (at 720)	139.94 (at 490)
12	n.d. (at 200)	13.64 (at 140
13	3.53 (at 370)	n.d. (at 250)
14	3.25 (at 1540)	291.19 (at 1040)
15	4.83 (at 202)	33.73 (at 144)

n.d., not detected; [a] concentrations for maximal effect measured are given in parentheses in μM; [b] concentrations for maximal effect measured are given in parentheses in μM.

Table S2. General values for prediction of physicochemical and ADME properties.

LogP	< –2.0	Very hydrophilic
	–2.0 to –1.0	Hydrophilic
	–1.0 to 4.2	Optimal
	4.2 to 5.0	Lipophilic
	> 5.0	Very lipophilic
Solubility	< 0.01	Highly insoluble
	0.01 to 0.10	Insoluble
	> 0.10	Soluble
Permeability	< 1.0	Poorly permeable
	1.0 to 7.0	Moderately permeable
	> 7.0	Highly permeable
PPB	< 10%	Not bound
	10% to 40%	Weakly bound
	40% to 80%	Moderately bound
	80% to 90%	Strongly bound
	> 90%	Extensively bound
CNS	< –3.5	Nonpenetrant
	–3.50 to –3.0	Weakly penetrant
	> –3.0	Penetrant